NASA TECHNICAL MEMORANDUM

NASA TM X-1204

NASA TM X-1204

EXPERIMENTAL COMPARISON OF APOLLO AFTERBODY HEATING IN AIR AND CO_2

by Clifford M. Akin

Ames Research Center

Moffett Field, Calif.

NATIONAL AERONAUTICS AND SPACE ADMINISTRATION • WASHINGTON, D. C. • JANUARY 1966

EXPERIMENTAL COMPARISON OF APOLLO AFTERBODY HEATING IN AIR AND CO_2

By Clifford M. Akin

Ames Research Center
Moffett Field, Calif.

NATIONAL AERONAUTICS AND SPACE ADMINISTRATION

[redacted] CLASSIFIED

EXPERIMENTAL COMPARISON OF APOLLO AFTERBODY HEATING IN AIR AND CO_2*

By Clifford M. Akin
Ames Research Center

SUMMARY

12700

Convective heat transfer was measured on the afterbody of an Apollo-like configuration in air and CO_2, at several angles of attack. The tests were made in a combustion driven shock tunnel at enthalpies sufficient to cause the gases to dissociate. No significant difference between the air and CO_2 results was observed. A stream-tube analysis for the tests indicated the inviscid flow over the afterbody was out of equilibrium which is a possible explanation of the observed results.

Author

INTRODUCTION

High-drag configurations, such as the Apollo, are being considered for probes to near planets. The atmosphere of these near planets is believed to contain varying amounts of carbon dioxide. As a first step to answering questions regarding the afterbody heating in the presence of these atmospheres, heat-transfer tests on the Apollo afterbody in pure carbon dioxide, for a range of angles of attack, were performed in the Ames 1-foot shock tunnel. The purpose of this report is to present these data and to compare them with air data at approximately the same enthalpy.

SYMBOLS

a	skin thickness of model
C_p	specific heat of the model material
H	enthalpy
p	pressure
q_w	wall heat-transfer rate
R	body radius (fig. 1)
R_c	corner radius (fig. 1)
R_n	nose radius (fig. 1)

[redacted]

[redacted]

T	temperature
u	velocity in streamwise direction
[XN]	ratio of number of nitrogen atoms to the total number of available nitrogen atoms
[XO]	ratio of number of oxygen atoms to the total number of available oxygen atoms
$[XO]_{qe}$, $[XN]_{qe}$	quasi-equilibrium atom fractions based on the nonequilibrium temperature
x	distance along body surface in streamwise direction from the body center line
Z	ratio of number of moles of gas to original number of cold moles
α	angle of attack (fig. 1)
θ	time
ρ	density of the model material

Subscripts

e	value at outer edge of the boundary layer
o	stagnation-point values
t	total stream conditions if it were isentropically brought to rest
w	wall value
∞	free-stream value

MODEL, INSTRUMENTATION, AND DATA REDUCTION

The model used in these tests is shown in figure 1. The shape is very similar to that of the Apollo command module. It was constructed with a 0.010-inch-thick 301 stainless steel afterbody. In an attempt to reduce sting interference, the model was mounted on a sting which came out of the model afterbody at an angle 30° from the model axis. Number 36 gauge chromel-constantan thermocouples were spot welded to the inside of the skin on the windward side.

The heat-transfer data were obtained by measuring the temperature response of the thin-skinned afterbody. The equation governing the data reduction was

$$q_w = \rho C_p a \frac{dT}{d\theta}$$

The thermocouple outputs were amplified and read out on a high-speed recording oscillograph (160 in./sec). These traces were curve fitted with polynomials, differentiated on a digital computer, and used in the above equation to obtain the heat-transfer rate. The data used were taken between 14 and 24 milliseconds after the start of a run, when the traces appeared linear. The maximum estimated error was ±10 percent of the heat-transfer rate.

The wall heat-transfer rates were normalized by the estimated Apollo stagnation-point heat transfer at $\alpha = 0^\circ$, $(q_w)_{o_{\alpha=o}}$. This was obtained by multiplying the measured stagnation-point heating rate on a 1-inch-diameter hemisphere, tested along with the Apollo model outside its bow shock, by $1.14\sqrt{R_{hemisphere}/R_n}$. This accounts for the difference in velocity gradients on the hemisphere and the Apollo model. (The factor 1.14 was taken from reference 1 and accounts for the effect on the velocity gradient, due to the Apollo model being a segment of a hemisphere.)

FACILITY AND TEST CONDITIONS

The facility is described in reference 2, and shown schematically in figure 2. The nominal test conditions were:

Gas	H_t, Btu/lb	p_t, atm	u_∞, ft/sec	p_o, atm	Ze_o, equil
Air	4500	285	13,000	0.15	1.23
CO_2	5400	285	12,000	.14	1.75

The test parameters p_o and p_t were measured and the others were calculated. The stagnation enthalpy was calculated by solving the conservation equations (energy, momentum, and mass) across the incident and reflected normal shocks in the driven section of the shock tunnel (see fig. 2). The inputs were the measured values of initial driven section pressure and incident shock velocity, along with the thermodynamic data for each gas. Thermodynamic data for carbon dioxide were calculated by H. Bailey (ref. 3). The final results were the pressure, temperature, and enthalpy in the stagnation region behind the reflected shock. It was found that the measured pressure behind the reflected shock was higher than the calculated value; therefore, the final stagnation enthalpy was obtained by assuming an isentropic compression from the calculated reflected shock pressure to the measured pressure (p_t). This increased the total enthalpy by approximately 10 percent.

Measurements of test-section static pressure in air and CO_2 indicated that the test streams in these gases were not in equilibrium. The Mach number and test-section velocity were determined by matching the total and static pressure measurements in air to those calculated in reference 4 for the

stagnation enthalpy and the effective area ratio obtained from a mass-flow-probe measurement. Conditions of frozen chemistry and vibrations were used to obtain the best match.

For carbon dioxide, information similar to that in reference 4 was not available, so the gas was assumed to be fully excited vibrationally and chemically frozen at the stagnation conditions of pressure and enthalpy. The free-stream velocity was then estimated from the effective nozzle area ratio for air.

RESULTS AND DISCUSSION

Figure 3 shows the heat-transfer distribution measured on the Apollo afterbody at several angles of attack in air and carbon dioxide. At $\alpha = 0^\circ$, the heat-transfer distribution changes very little with x/R indicating that the flow was probably separated. As angle of attack increases, the heat transfer increases and becomes progressively more dependent on x/R until at the higher angles of attack ($\alpha = 33^\circ$ and 44°) the distribution on the windward side is characteristic of attached flow (see ref. 5). Small differences are found between the air and carbon dioxide distributions where direct comparison can be made ($\alpha = 0^\circ$ and 33°). At $\alpha = 0^\circ$ the carbon dioxide heat-transfer distribution is slightly greater than in air, while at 33° any difference seems to be within the scatter of the data. At $\alpha = 16^\circ$, 23°, and 44°, no air data were obtained; however, the good agreement at $\alpha = 0^\circ$ and 33° would suggest similar comparisons at the other angles.

Prior to these tests, it was anticipated that there might be large differences in the heat transfer for air and carbon dioxide. This was concluded from unpublished calculations, performed as in reference 6, which showed the pressures in carbon dioxide to be 50 percent lower than those in air on the afterbody of a hemisphere cylinder for equilibrium flow. It was felt that a similar result might exist for the Apollo afterbody. The fact that the differences between air and carbon dioxide were small could be explained by nonequilibrium effects on the inviscid flow over the Apollo afterbody. If the inviscid flow is frozen, the isentropic exponents of the gases are about the same and the expansion around the corner would result in comparable afterbody pressure and heat-transfer distributions. To determine if the inviscid flow over the Apollo afterbody were frozen, a calculation which showed the chemical species fractions in a stream-tube over the windward side of the afterbody was carried out and the results are presented next.

Figure 4 shows the chemical species fractions in a stream-tube plotted against x/R for the Apollo at 33° angle of attack in air. This stream-tube may be visualized as very near the outer edge of the boundary layer in the inviscid flow. In figure 4 the atomic species of oxygen [XO] starts at zero, because of an assumption that no initial dissociation occurs across the shock wave, and rapidly approaches the quasi-equilibrium value of oxygen $[XO]_{qe}$. When [XO] equals $[XO]_{qe}$, the oxygen is considered to be in thermochemical equilibrium. There is also a slight amount of nitrogen dissociation [XN]

during the initial high-temperature portion of the streamline. After about $x/R = 1.11$, the chemical reactions proceed so slowly that [XO] becomes fixed, deviating from the quasi-equilibrium value, and remains so over the afterbody, whereas the nitrogen recombines fast enough to maintain itself in equilibrium, $[XN] = [XN]_{qe}$. Thus for air, the inviscid flow is believed frozen over the windward side at $\alpha = 33^{\circ}$. Similar results were found for $\alpha = 0^{\circ}$. No similar stream-tube calculation exists for carbon dioxide; however, it is expected that the carbon dioxide inviscid flow is also not in equilibrium, since carbon dioxide recombination rates are even slower than those for air.

CONCLUDING REMARKS

On the Apollo afterbody no significant difference was observed in heat-transfer distributions obtained in air and CO_2 at angles of attack of 0° and 33°. This may be the result of nonequilibrium effects in the inviscid flow field about the Apollo model.

Ames Research Center
National Aeronautics and Space Administration
Moffett Field, Calif., Aug. 2, 1965

REFERENCES

1. Marvin, Joseph G.; Tendeland, Thorval; and Kussoy, Marvin: Apollo Forebody Pressure and Heat-Transfer Distributions in Helium at $M_\infty = 20$. NASA TM X-854, 1963.

2. Cunningham, Bernard E.; and Kraus, Samuel: A 1-Foot Hypervelocity Shock Tunnel in Which High-Enthalpy, Real-Gas Air Flows Can Be Generated With Flow Times of About 180 Milliseconds. NASA TN D-1428, 1962.

3. Bailey, Harry E.: Equilibrium Thermodynamic Properties of Carbon Dioxide. NASA SP 3014, 1965.

4. Yoshikawa, Kenneth K.; and Katzen, Elliott D.: Charts for Air-Flow Properties in Equilibrium and Frozen Flows in Hypervelocity Nozzles. NASA TN D-693, 1961.

5. Jones, Robert A.: Experimental Investigation of the Overall Pressure Distribution, Flow Field, and Afterbody Heat-Transfer Distribution of an Apollo Reentry Configuration at a Mach Number of 8. NASA TM X-813, 1963.

6. Inouye, Mamoru; Rakich, John V.; and Lomax, Harvard: A Description of Numerical Methods and Computer Programs for Two-Dimensional and Axisymmetric Supersonic Flow Over Blunt-Nosed and Flared Bodies. NASA TN D-2970, 1965.

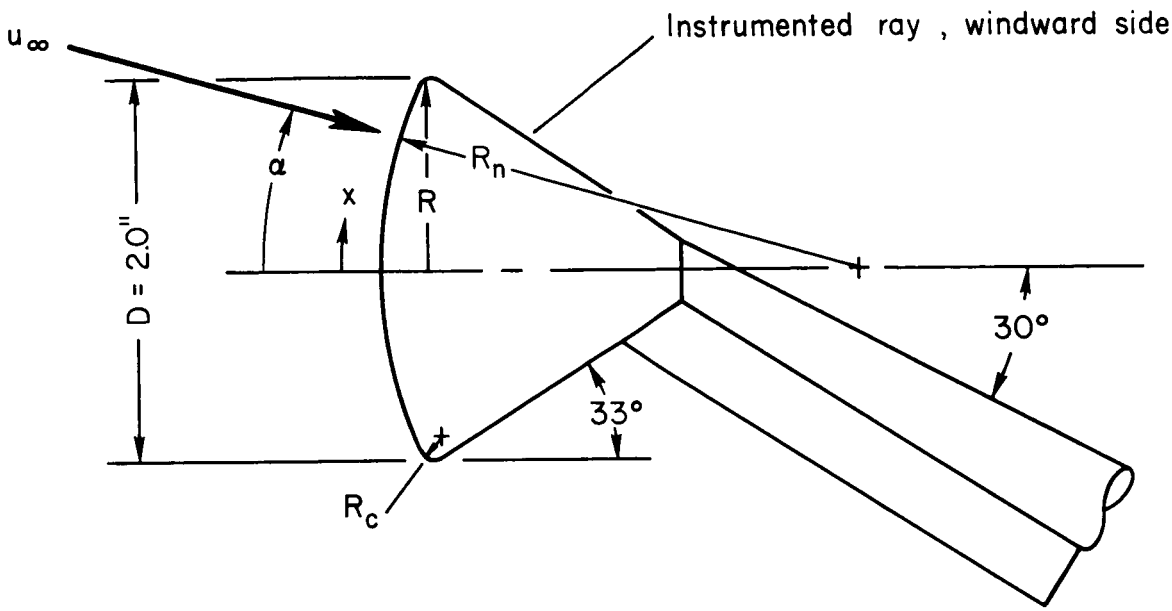

R_n = 1.25 D

R_c = .052 D

Figure 1.- Apollo configuration heat-transfer model.

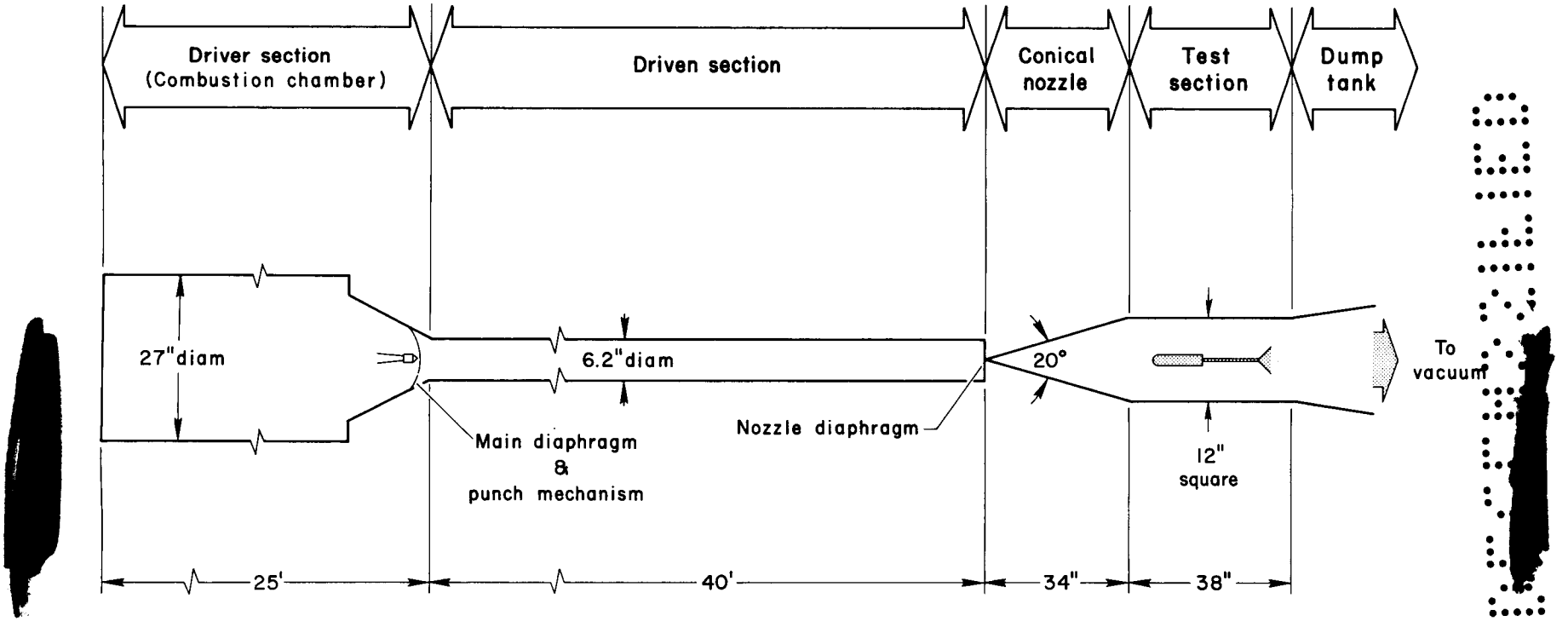

Figure 2.- Schematic drawing of Ames 1-foot shock tunnel.

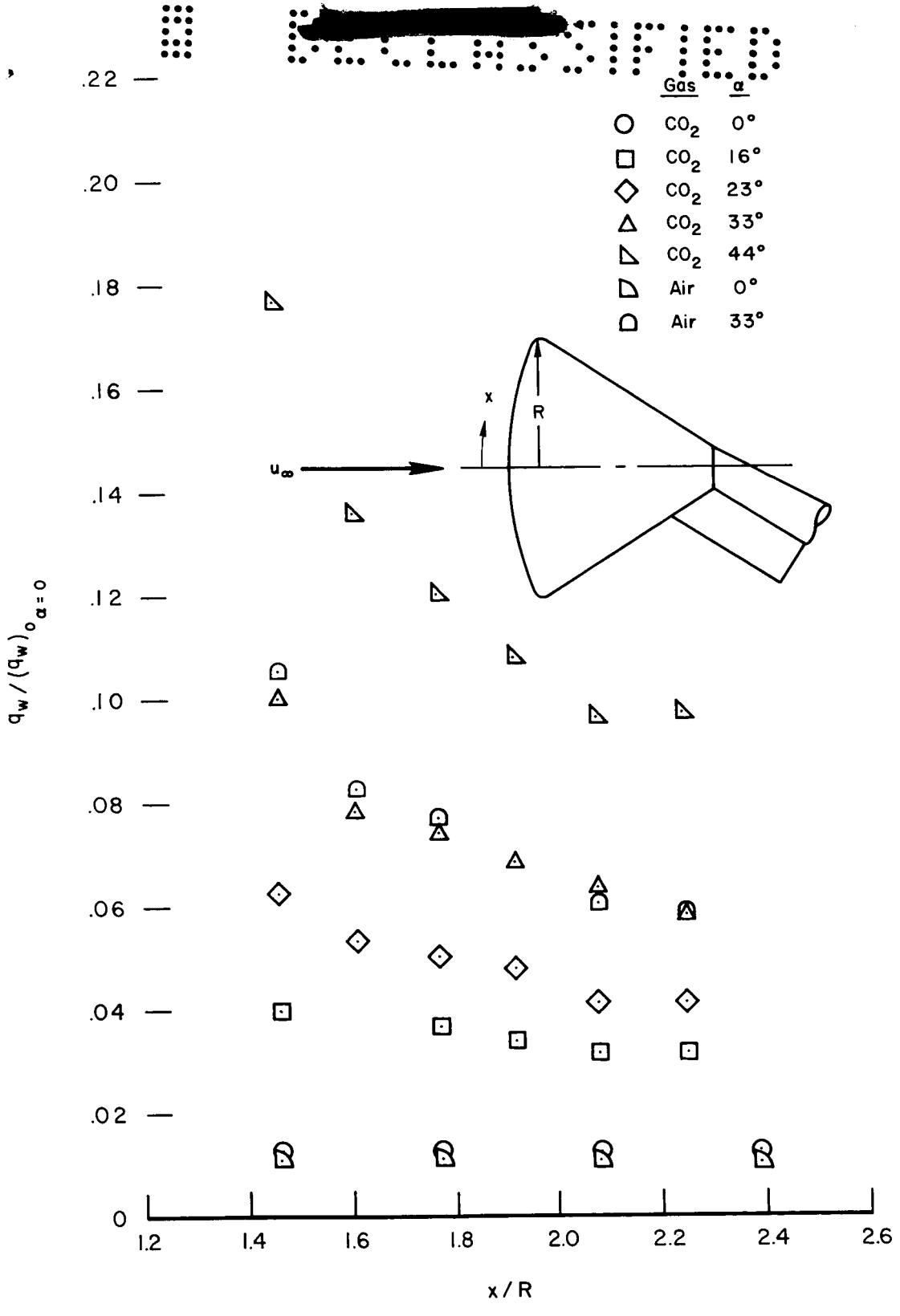

Figure 3.- Comparison of air-CO_2 afterbody heat-transfer distributions.

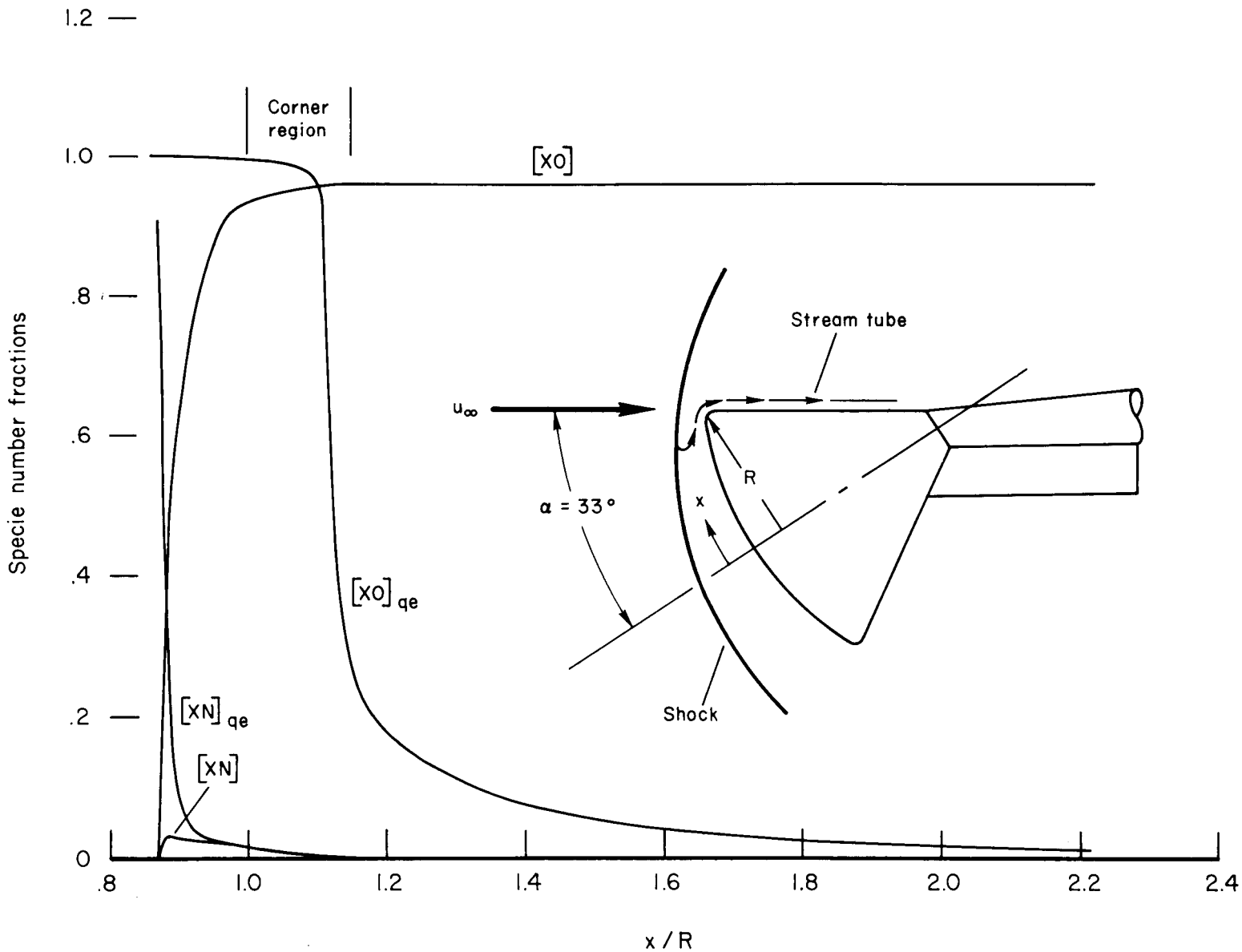

Figure 4.- Nonequilibrium streamtube calculation, $\alpha = 33^{\circ}$.